ISSN 1063-7834, Physics of the Solid State, 2015, Vol. 57, No. 12, pp. 2410–2416. © Pleiades Publishing, Ltd., 2015.
Original Russian Text © M. Budzynski, V.I. Val'kov, A.V. Golovchan, V.I. Mityuk, Z. Surowiec, T.M. Tkachenko, 2015, published in Fizika Tverdogo Tela, 2015, Vol. 57, No. , pp. –.

MAGNETISM

Structure and Properties of $MnNi_{1-x}Fe_xGe$ ($0.10 \leqslant x \leqslant 0.25$)

M. Budzynski[a], V. I. Val'kov[b], A. V. Golovchan[b], V. I. Mityuk[c,*], Z. Surowiec[a], and T. M. Tkachenko[c]

[a] *Institute of Physics, Maria Curie-Sklodowska University, pl. Marii Curie-Sklodowskiej 1, Lublin, 20-031 Poland*

[b] *Donetsk Institute of Physics and Engineering named after O. O. Galkin, National Academy of Sciences of Ukraine, ul. R. Luxemburg 72, Donetsk, 83114 Ukraine*

[c] *Scientific and Practical Materials Research Center, National Academy of Sciences of Belarus, ul. P. Brovki 19, Minsk, 220072 Belarus*

* *e-mail: mitsiuk@physics.by*

Received May 25, 2015

Abstract—The magnetic and structural characteristics of the solid solutions $MnNi_{1-x}Fe_xGe$ ($0.10 \leqslant x \leqslant 0.25$) have been investigated. At $T = 290$ K, the solid solutions have a hexagonal structure of the Ni_2In type. The magnetic properties of $MnNi_{1-x}Fe_xGe$ ($0.10 \leqslant x \leqslant 0.25$) weakly depend on the type of heat treatment. Based on the magnetometric and Mössbauer data, it has been found that, in the solid solutions $MnNi_{1-x}Fe_xGe$ ($0.10 \leqslant x \leqslant 0.25$) with iron concentrations $x = 0.10$–0.15, the iron atoms are statistically distributed over the octahedral and trigonal-bipyramidal positions. At concentrations above $xx = 0.15$, iron atoms replace only the manganese atoms in the octahedral positions, whereas nickel atoms in the trigonal-bipyramidal positions are not replaced by the iron atoms.

DOI: 10.1134/S1063783415120094

1. INTRODUCTION

Considerable interest expressed by many researchers in the half-Heusler alloys $MnNi_{1-x}Fe_xGe$ has been associated with the existence of a wide variety of magnetic phases and the occurrence of structural and magnetostructural phase transitions in these materials, which are accompanied by significant magnetocaloric and magnetostrictive effects [1–4]. On the one hand, the possibility of using the magnetocaloric effect and magnetostriction in the fabrication of effective magnetic refrigerators and magnetostrictors makes the $MnNi_{1-x}Fe_xGe$ system attractive for practical applications. On the other hand, the investigation of specific features of the mechanism of giant spontaneous magnetostriction occurring in the $MnNi_{1-x}Fe_xGe$ alloys during magnetostructural phase transitions is a fundamental problem in the physics of magnetic phenomena. Indeed, in contrast to the $Mn_{2-x}Fe_xAs_{0.5}P_{0.5}$ system, in which the spontaneous magnetostriction is associated with the destruction of the magnetic moment of iron atoms due to the disappearance of the magnetic order [5], the spontaneous magnetostriction in the $MnNi_{1-x}Fe_xGe$ system, according to preliminary first-principles calculations, is not related to the change in local magnetic characteristics of the 3*d* ions. It can only be assumed that the anisotropic change in the lattice parameters (from +10% along the hexagonal axis to –7% in the basal plane) [2], which occurs during the magnetic ordering in the $MnNi_{1-x}Fe_xGe$ system, is a consequence of the superposition of the magnetic and structural phase transitions observed in the ternary system MnNiGe.

The structural and magnetic properties of the ternary compounds MnFeGe and MnNiGe were investigated previously. In [6], it was shown that the MnFeGe compound crystallizes into a hexagonal structure of the Ni_2In type (space group $P6_3/mmc$) over the entire temperature range. The results of the neutron diffraction investigations of $Mn_{0.95}Fe_{1.0}Ge$ powders demonstrated that the magnetic moments of manganese atoms at temperatures below 240 K are antiferromagnetically ordered, whereas the magnetic moments of iron atoms are ferromagnetically ordered [7]. At the same time, the MnNiGe compound at room temperature has an orthorhombic structure of the TiNiSi type (space group *Pnma*) [8, 9]. Below the Néel temperature ($T_N = 346$ K), this compound is a helical antiferromagnet. At the temperature $T_{d,h} = 528$ K, the MnNiGe compound undergoes a first-order displacive phase transition from the low-temperature orthorhombic structure of the TiNiSi type to the high-temperature hexagonal structure of the Ni_2In type. This transition is accompanied by a large temperature hysteresis ($T_{d,h} - T_{d,0} = 45$ K), as well as by giant anisotropic changes in the parameters and volume of the lattice ($\Delta c_h/c_h \approx -10\%$, $\Delta a_h/a_h \approx +7\%$, $\Delta V_h/V_h \approx -3\%$). Similar structural transitions are

Table 1. Magnetic characteristics of the solid solutions $MnNi_{1-x}Fe_xGe$ ($0.10 \leqslant x \leqslant 0.25$)

Sample no.	Composition	Heat treatment	T_C, K	σ, emu/g
1	$MnNi_{0.75}Fe_{0.25}Ge$	"Quenching on wheel"	234	67.60
2	$MnNi_{0.8}Fe_{0.2}Ge$	The same	232	63.68
3	$MnNi_{0.85}Fe0.15Ge$	»	220	62.86
4	$MnNi_{0.9}Fe_{0.1}Ge$	»	218	56.73
5	$MnNi_{0.75}Fe_{0.25}Ge$	Quenching + annealing (T – 850 °C, t = 6 h)	232	65.18
6	$MnNi_{0.80}Fe_{0.20}Ge$	The same	230	65.95
7	$MnNi_{0.85}Fe_{0.15}Ge$	»	219	59.61
8	$MnNi_{0.9}Fe_{0.1}Ge$	»	295	10.93

accompanied by a change in the period of the unit cell and are described by a softening of one of the phonon modes [10], which in MnNiGe, as in MnAs [11], can be stimulated by a strong electron–phonon interaction. This assumption is confirmed by the following fact. Upon the substitution of iron for nickel in MnNiGe, already at room temperature this alloys crystallizes into the hexagonal phase; i.e., the structural transition temperatures $T_{d,\ h}$ and $T_{d,\ 0}$ significantly decrease [8]. Since the ionic radii of nickel and iron are close to each other (1.24 and 1.25 nm, respectively), such a significant change in the structural transition temperature apparently is associated with a decrease in the electronic filling of the 3*d* band and, consequently, with a change in the electron–phonon coupling.

The electronic structure of the four-component MnNiFeGe system has been poorly studied for different concentrations and distributions of 3*d* components as well as for different degrees of filling of the 3*d* bands in $MnNi_{1-x}Fe_xGe$.

In this work, we have investigated the structural, magnetic, and Mössbauer properties of solid solutions in the $MnNi_{1-x}Fe_xGe$ system with compositions in the iron concentration range $0.10 \leqslant x \leqslant 0.25$ for the purpose of obtaining useful information for the elucidation of the mechanisms of the formation of magnetostructural phases and their role in the appearance of a giant magnetostriction.

2. SAMPLE PREPARATION AND EXPERIMENTAL TECHNIQUE

Samples of $MnNi_{1-x}Fe_xGe$ solid solutions with four different compositions (x = 0.10, 0.15, 0.20, and 0.25) were prepared from a melt of homogeneous mixtures of powders with a purity of no lower than 99.99% in an argon atmosphere, followed by a rapid quenching from the liquid state onto a wheel rotating at a linear velocity of 20 mm/s ("quenching on wheel"). Some of the synthesized samples of each composition were then annealed at the temperature T = 850°C for 6 h.

The X-ray powder diffraction analysis, which was performed on powder samples in the CuK_α radiation, demonstrated that all the prepared $MnNi_{1-x}Fe_xGe$ solid solutions with compositions in the iron concentration range $0.10 \leqslant x \leqslant 0.25$ crystallized into a hexagonal structure of the Ni_2In type (space group $P6_3/mmc$) (Fig. 1).

The specific magnetization of the solid solutions $MnNi_{1-x}Fe_xGe$ ($0.10 \leqslant x \leqslant 0.25$) was measured by the Faraday method in a magnetic field of 0.86 T at temperatures in the range 77 K $\leqslant T \leqslant$ 500 K. The Curie temperatures were determined by the extrapolation of a linear part of the temperature dependence of the square of the specific magnetization to the temperature axis. The obtained values of specific magnetizations σ and Curie temperatures T_C are presented in Table 1.

In order to elucidate the character of the distribution of metal atoms over the sublattices, we carried out the Mössbauer investigations of the synthesized solid solutions $MnNi_{1-x}Fe_xGe$ ($0.10 \leqslant x \leqslant 0.25$). The Mössbauer experiment was performed in the conventional transmission geometry in the constant acceleration mode using a source of 57mFe/Rh resonant radi-

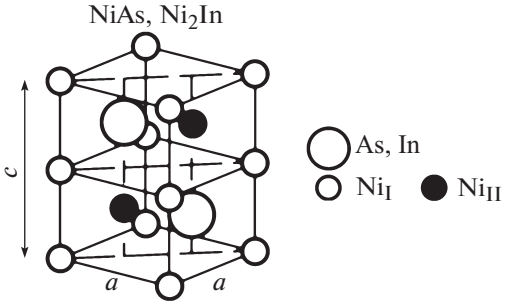

Fig. 1. Structure of the Ni_2In type.

Table 2. Parameters of the Mössbauer spectra of the quenched samples $MnNi_{1-x}Fe_xGe$ ($0.10 \leqslant x \leqslant 0.25$)

Sample no.	Composition	First subspectrum				Second spectrum			
		IS_1, mm/s	QS_2, mm/s	Γ_2, mm/s	C_2, rel. units	IS_1, mm/s	QS_2, mm/s	Γ_2, mm/s	C_2, rel. units
1	$MnNi_{0.75}Fe_{0.25}Ge$ (quenching)	0.259	0.731	0.126	0.673	0.477	0.595	0.188	0.327
2	$MnNi_{0.8}Fe_{0.2}Ge$ (quenching)	0.248	0.693	0.132	0.600	0.476	0.570	0.171	0.400
3	$MnNi_{0.85}Fe_{0.15}Ge$ (quenching)	0.241	0.679	0.135	0.479	0.462	0.498	0.183	0.521
4	$MnNi_{0.9}Fe_{0.1}Ge$ (quenching)	0.235	0.639	0.154	0.469	0.477	0.477	0.166	0.531
5	$MnNi_{0.75}Fe_{0.25}Ge$ (quenching + annealing)	0.257	0.739	0.123	0.767	0.479	0.570	0.169	0.233
6	$MnNi_{0.8}Fe_{0.2}Ge$ (quenching + annealing)	0.245	0.693	0.134	0.675	0.493	0.576	0.156	0.325
7	$MnNi_{0.85}Fe_{0.15}Ge$ (quenching + annealing)	0.235	0.675	0.146	0.603	0.476	0.524	0.152	0.397
8	$MnNi_{0.9}Fe_{0.1}Ge$ (quenching + annealing)	0.240	0.684	0.132	0.582	0.510	0.537	0.159	0.418

The isomer shift IS is given with respect to ^{57}Fe.

Table 3. Parameters of the Mössbauer spectra of the $MnNi_{1-x}Fe_xGe$ samples at $T = 77$ K

Sample no.	Composition	IS_1, mm/s	IS_2, mm/s	QS_1, mm/s	QS_2, mm/s	H_1, rel. units	H_2, rel. units	Γ_1, mm/s	Γ_2, mm/s	C_1, rel. units	C_2, rel. units
3	$MnNi_{0.85}Fe_{0.15}Ge$ (quenching)	0.264	0.470	−0.312	−0.370	12.7	12.3	0.21	0.20	0.479	0.521
1	$MnNi_{0.75}Fe_{0.25}Ge$ (quenching)	0.344	0.489	−0.317	−0.450	12.3	11.8	0.21	0.20	0.673	0.327
5	$MnNi_{0.75}Fe_{0.25}Ge$ (quenching + annealing)	0.340	0.489	−0.338	−0.454	12.2	11.7	0.22	0.19	0.767	0.233

ation with a line width of 0.11 mm/s. The temperatures of the absorber were equal to 77 and 290 K. The Mössbauer spectra of the samples at temperatures $T = 290$ and 77 K are shown in Figs. 2 and 3, respectively. Tables 2 and 3 present the following refined parameters of the spectra: IS is the isomer shift of the subspectrum with respect to metallic iron at room temperature, QS is the quadrupole splitting, and Γ is the line width.

3. RESULTS AND DISCUSSION

The performed analysis of the temperature dependences of the specific magnetization revealed that samples of all the studied compositions $MnNi_{1-x}Fe_xGe$ ($0.10 \leqslant x \leqslant 0.25$) are ferromagnets. Neither phase transitions of the antiferromagnet–ferromagnet type nor significant dependence of the magnetic properties on the heat treatment of the alloys were found. The obtained values of specific magnetizations and Curie temperatures for samples of the same composition after different heat treatments (quenching and quenching with annealing) differ only slightly from each other. After the additional annealing of the samples, the specific magnetization decreases insignificantly (by no more than 2 emu/g), while the Curie temperature decreases by ~1–2 K. The small decrease in the magnetic parameters during the annealing of the samples can be associated with the specific features of the Ni_2In-type structure (Fig. 1). Metalloid atoms (in our case, germanium atoms) form a close-packed hexagonal framework, in which there are two types of positions occupied by metal atoms, namely, the octahedral (*Me*I) positions 2*a* and the trigonal-bipyramidal (*Me*II) positions 2*d*. In our case, these two types of structurally nonequivalent positions

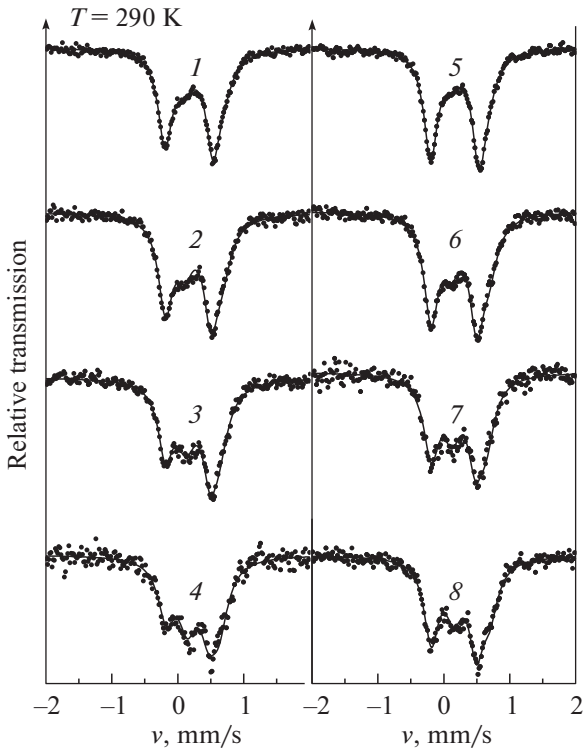

Fig. 2. Mössbauer spectra of the samples $MnNi_{1-x}Fe_xGe$ ($0.10 \leqslant x \leqslant 0.25$) at room temperature. The numbers of the curves correspond to the numbers of the samples in Table 2.

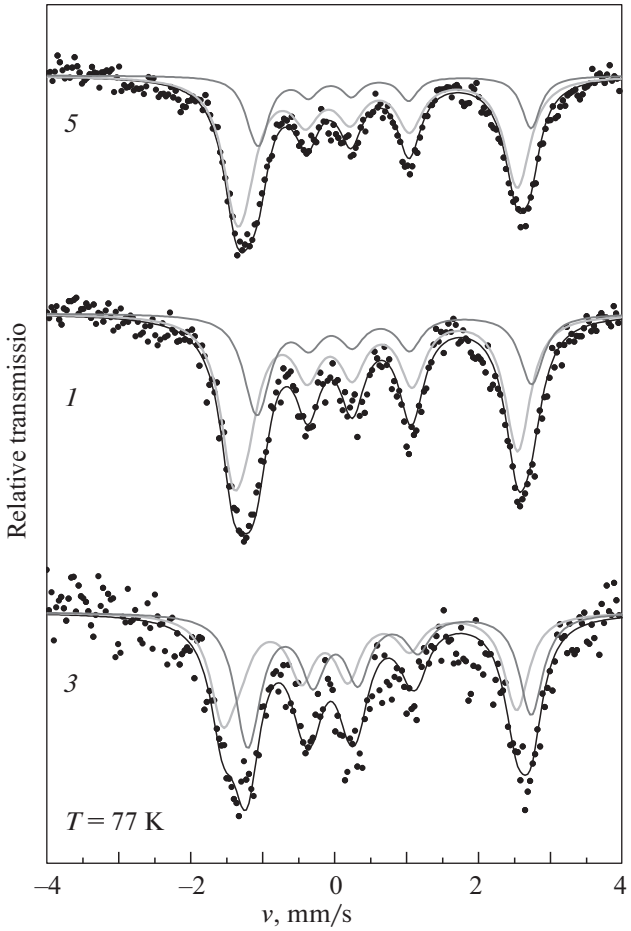

Fig. 3. Mössbauer spectra of the $MnNi_{1-x}Fe_xGe$ samples at 77 K: (*1*) $MnNi_{0.75}Fe_{0.25}Ge$ (quenching), (*3*) $MnNi_{0.85}Fe_{0.15}Ge$ (quenching), and (*5*) $MnNi_{0.75}Fe_{0.25}Ge$ (quenching + annealing).

can be occupied by metal atoms of three types, namely, manganese, nickel, and iron atoms. The properties of the alloy as a whole depend on the manner in which metal atoms are distributed over the aforementioned positions. The structure of this type is characterized by a high degree of imperfection, especially when the alloy was synthesized under the conditions of "quenching on wheel." It is believed [5, 8] that, in similar three-component solid solutions with two types of metal atoms (MnFeGe and MnNiGe), the manganese atoms are located in the *Me*I positions, whereas the nickel (or iron) atoms occupy only the *Me*II positions. However, the authors of [5] assumed that, for the MnFeGe compound with the Ni_2In-type structure, there is a possibility of mutual "mixing" (up to 17 at %) of atoms in the sublattices *Me*I and *Me*II. In our case, the distribution of Mn, Ni, and Fe atoms over the positions of the structure can be more complex. The quenching leads to an increase in the degree of imperfection of the $MnNi_{1-x}Fe_xGe$ solid solutions with the Ni_2In-type structure. It seems likely that, upon quenching, in the sublattices there is a certain amount of vacant structural positions. In turn, the subsequent annealing leads to a "regularization" of the alloy, during which holes are filled with atoms. Since the amount of nickel in the calculation formula is less than the total amount of manganese and iron, the Fe and Mn atoms in the case of the completely filled *Me*I sublattice partially occupy the *Me*II sublattice. From the literature, it is known that, in the *Me*II sublattice, the magnetic moment is not localized at the nickel atoms. Some of the magnetic atoms of iron and manganese, after they passed into the *Me*II sublattice, apparently also cease to participate in the magnetic interaction, thereby somewhat decreasing the total magnetization of the alloy.

However, if we consider the case where the magnetization of the $MnNi_{1-x}Fe_xGe$ solid solutions changes with an increase in the iron concentration x in the samples subjected to the same heat treatment, it turns out that an increase in the iron concentration leads to an increase in the magnetization. This means that, after the replacement of a limiting number of atoms in the *Me*II sublattice at $x \sim 0.20$, the iron atoms with a further increase in their concentration in the solid solution occupy only the *Me*I positions by replacing the manganese atoms.

Table 4. Hyperfine magnetic fields H_{hf} calculated using the fully relativistic Korringa–Kohn–Rostoker method

Alloy	$M(Mn_I)$, μ_B	$M(Fe_I)$, μ_B	H_{hfII}, T	$M(Mn_{II})$, μ_B	$M(Fe_{II})$, μ_B	H_{hfII}, T	$M_{f.u.}$, μ_B	E_{tot}, Ry/f.u.
Hexagonal structure of the Ni_2In type, $a = 4.0956$ Å, $c = 5.355$ Å								
LDA approximation, nonmagnetic state								
$(Mn_{0.86}Fe_{0.14})_I(Ni_{0.85}Fe_{0.01}\ Mn_{0.14})_{II}Ge$	–	–	–	–	–	–	–	–9468.06075
$(Mn_{0.99}Fe_{0.01})_I(Ni_{0.85}Fe_{0.14}\ Mn_{0.01})_{II}Ge$	–	–	–	–	–	–	–	–9468.06159
GGA approximation, nonmagnetic state								
$(Mn_{0.86}Fe_{0.14})_I(Ni_{0.85}Fe_{0.01}\ Mn_{0.14})_{II}Ge$	–	–	–	–	–	–	–	–9482.84201
$(Mn_{0.95}Fe_{0.05})_I(Ni_{0.85}Fe_{0.10}\ Mn_{0.05})_{II}Ge$	–	–	–	–	–	–	–	–9482.84255
LDA approximation, ferromagnetic state								
$(Mn_{0.86}Fe_{0.14})_I(Ni_{0.85}Fe_{0.01}Mn_{0.14})_{II}Ge$	2.71	2.26	−14.4	0.91	1.19	−15.5	2.78	–9468.08958
$(Mn_{0.99}Fe_{0.01})_I(Ni_{0.85}Fe_{0.14}Mn_{0.01})_{II}Ge$	2.71	2.27	−14.5	0.26	1.0	−15.8	2.83	–9468.09353
GGA approximation, ferromagnetic state								
$(Mn_{0.86}Fe_{0.14})_I(Ni_{0.85}Fe_{0.01}Mn_{0.14})_{II}Ge$	2.98	2.44	−17.1	1.58	1.42	−17.0	3.12	–9482.87981
$(Mn_{0.95}Fe_{0.05})_I(Ni_{0.85}F_{e0.10}Mn_{0.05})_{II}Ge$	3.0	2.47	−17.2	1.15	1.33	−17.6	3.14	–9482.88268
Orthorhombic structure of the TiNiSi type TiNiSi, $a = 6.01$, $b = 3.744$ Å, $x(Mn) = 0.031$, $z(Mn) = 0.185$, $x(Ni) = 0.147$, $z(Ni) = 0.557$, $x(Ge) = 0.758$, $z(Ge) = 0.623$								
LDA approximation, ferromagnetic state								
$(Mn_{0.86}Fe_{0.14})_I(Ni_{0.85}Fe_{0.01}Mn_{0.14})_{II}Ge$	2.84	2.24	−13.5	2.22	1.75	−20.5	3.10	–9468.19401
$(Mn_{0.99}Fe_{0.01})_I(Ni_{0.85}Fe_{0.14}Mn_{0.01})_{II}Ge$	2.84	2.25	−14.1	2.21	1.73	−21.7	3.10	–9468.19938
GGA approximation, ferromagnetic state								
$(Mn_{0.86}Fe_{0.14})_I(Ni_{0.85}Fe_{0.01}Mn_{0.14})_{II}Ge$	2.97	2.33	−14.7	2.37	1.82	−22.9	3.18	–9482.98647
$(Mn_{0.95}Fe_{0.05})_I(Ni_{0.85}Fe_{0.10}Mn_{0.05})_{II}Ge$	2.97	2.33	−15.1	2.36	1.81	−23.8	3.17	–9482.99038
Hexagonal structure of the Ni_2In type, $a = 4.067$ Å, $c = 5.327$ Å								
LDA approximation, nonmagnetic state								
$(Mn_{0.8}Fe_{0.2})_I(Ni_{0.75}Fe_{0.05}\ Mn_{0.2})_{II}Ge$	–	–	–	–	–	–	–	–9418.5017
$(Mn_{0.99}Fe_{0.01})_I(Ni_{0.75}Fe_{0.24}\ Mn_{0.01})_{II}Ge$	–	–	–	–	–	–	–	–9418.5032
GGA approximation, nonmagnetic state								
$(Mn_{0.8}Fe_{0.2})_I(Ni_{0.75}Fe_{0.05}\ Mn_{0.2})_{II}Ge$	–	–	–	–	–	–	–	–9433.2354
$(Mn_{0.99}Fe_{0.01})_I(Ni_{0.75}Fe_{0.24}\ Mn_{0.01})_{II}Ge$	–	–	–	–	–	–	–	–9433.2368
LDA approximation, ferromagnetic state								
$(Mn_{0.8}Fe_{0.2})_I(Ni_{0.75}Fe_{0.05}Mn_{0.2})_{II}Ge$	2.59	2.18	14.5	1.25	1.25	14.4	2.81	–9418.52806
$(Mn_{0.99}Fe_{0.01})_I(Ni_{0.75}Fe_{0.24}Mn_{0.01})_{II}Ge$	2.61	2.20	14.6	0.74	1.03	15.2	2.84	–9418.5336
GGA approximation, ferromagnetic state								
$(Mn_{0.8}Fe_{0.2})_I(Ni_{0.75}Fe_{0.05}Mn_{0.2})_{II}Ge$	2.83	2.36	17.2	1.63	1.43	16.0	3.1	–9433.27012
$(Mn_{0.99}Fe_{0.01})_I(Ni_{0.75}Fe_{0.24}Mn_{0.01})_{II}Ge$	2.87	2.39	17.3	0.58	1.2	17.1	3.11	–9433.2759

The only composition for which there is a significant discrepancy between the curves of the temperature dependences of the magnetization for the samples subjected to different heat treatments is the composition with an iron concentration of 10 at % (i.e., it is the $MnNi_{0.9}Fe_{0.1}Ge$ compound). The X-ray diffraction analysis revealed that it is a single-phase solid solution. After the additional annealing, the specific magnetization of the sample of this composition significantly decreases (from approximately 56 to ~10 emu/g), whereas the magnetic phase transition temperature T_C increases from 218 K in the quenched sample of the $MnNi_{0.9}Fe_{0.1}Ge$ composition to 295 K in the annealed sample.

The data obtained from the Mössbauer measurements make it possible to clarify the picture of the dis-

tribution of metal atoms over the sublattices. At T = 290 K, the solid solutions do not exhibit magnetic properties, and their spectra have the form of quadrupole split lines. Each Mössbauer spectrum (Fig. 2) is described by two subspectra in the form of quadrupole doublets, and each doublet corresponds to iron atoms in one of two possible crystallographic positions: *Me*I or *Me*II. The ratio of the concentrations of iron atoms in two metal sublattices can be roughly estimated from the ratio of the integrated intensities of the corresponding subspectra, i.e., from the relative contributions of the areas of the subspectra to the total spectrum (parameters C_1 and C_2 in Tables 2 and 3). It can be seen (Fig. 2, from bottom to top) that an increase in the iron concentration x leads to an increase in the relative concentration of iron atoms in one of the sublattices.

If the atomic distribution obtained above from the data of the magnetic measurements is considered to be accurate, the first subspectrum with an increasing contribution to the total area of the spectrum corresponds to iron atoms in the *Me*I (2*a*) sublattice. This subspectrum is characterized by lower values of the isomer shifts IS (~0.20 mm/s). The second subspectrum with a decreasing contribution to the total area of the spectrum (as the iron concentration x increases) and with higher values of the isomer shifts IS corresponds to iron atoms in the 2*d* (*Me*II) positions. An increase of the iron concentration in the $MnNi_{1-x}Fe_xGe$ alloy leads to an increase in the iron concentration in the 2*a* sublattice (octahedral positions). Moreover, this increase in the annealed samples is more significant: from 0.582(2*a*)/0.418(2*d*) for the composition with $x = 0.10$ to 0.767/0.233 for the composition with $x = 0.25$.

Thus, the magnetic and Mössbauer data obtained in this study indicate that, in the $MnNi_{1-x}Fe_xGe$ solid solutions with iron concentrations $x = 0.10$–0.15, the iron atoms are statistically distributed over the two structural sublattices *Me*I and *Me*II. With an increase in the iron concentration $x > 0.15$, the relative concentration of iron atoms in the *Me*II sublattice remains almost constant, whereas excessive iron atoms above this relative concentration replace only the manganese atoms in the *Me*I positions.

The Mössbauer spectra of the solid solutions at liquid-nitrogen temperature (Table 3, Fig. 3) have the form of magnetically split lines, which corresponds to the magnetic state of the solid solutions. The spectra were processed in the model of two sextets with close values of the hyperfine magnetic fields. It was found that, in the spectrum of each composition, the magnetic fields differ by no more than 0.5 T. In this case, it was assumed that the iron atoms located in two different structurally nonequivalent positions of the orthorhombic structure, which is characteristic of $MnNi_{1-x}Fe_xGe$ compounds at $T = 77$ K, give rise to the corresponding subspectra of the total spectrum. The width of lines in the sextets exceeds the natural line width, which can be explained by a nonideality of the crystal structure of the sample. As a result, the electric field gradient is oriented relative to the direction of magnetization in not the only way, which leads to a broadening of the lines in the sextet [12]. The differences in the heat treatments of the sample with the same composition have a weak effect on the hyperfine magnetic fields at the iron nuclei (shown for the $MnNi_{0.75}Fe_{0.25}Ge$ sample used as an example, Table 3).

The experimental data, which indicate close values of the hyperfine fields at the iron nuclei in different crystallographic positions, are not consistent with the results of the calculations performed in the present study (Table 4). The hyperfine fields H_{hf} were calculated using the fully relativistic Korringa–Kohn–Rostoker method [13] in the local density approximation (LDA/VWN) [14] and in the generalized gradient approximation (GGA/PBE) [15] for the exchange–correlation energy. For the crystal potential, we used the atomic sphere approximation.

The difference in the energies $\Delta E_{NM,hex}$ for different variants of the substitution of iron atoms for manganese or nickel atoms was calculated by using the example of the sample with the $MnNi_{0.85}Fe_{0.15}Ge$ composition at room temperature, i.e., in the nonmagnetic hexagonal phase. According to the results of these calculations, the iron atoms are characterized by an almost equiprobable distribution over the nickel and manganese positions (Table 4):

$$\Delta E_{NM,hex} = E[(Mn_{0.99}Fe_{0.01})_{2a}(Ni_{0.85}Fe_{0.14}Mn_{0.01})_{2c}Ge] - E[(Mn_{0.86}Fe_{0.14})_{2a}(Ni_{0.85}Fe_{0.01}Mn_{0.14})_{2c}Ge] = -132\,\text{K/f.u.}$$

The results of the calculations of the energy difference are confirmed by the experimental data. The ratio of the areas of two peaks in the Mössbauer spectrum of the $MnNi_{0.85}Fe_{0.15}Ge$ sample is equal to $C_2/C_1 = 0.521/0.479 = 1.09$. Since this distribution is nonequilibrium, the annealing of the sample leads to a redistribution of iron atoms over the crystallographic positions of the structure. For the annealed sample, the ratio of the areas of two peaks in the Mössbauer spectrum becomes equal to $C_2/C_1 = 0.397/0.603 = 0.66$ (Table 2).

The energy difference between the configurations of atoms increases in absolute value to $\Delta E_{NM,\,hex} = -623$ K/f.u. in the hexagonal ferromagnetic state and to $\Delta E_{NM,\,orth} = -846$ K/f.u in the orthorhombic phase. Therefore, the quenching of the sample can lead to a freezing of the "nonequilibrium" distribution of iron atoms over the nickel and manganese sublattices, as well as to a freezing of part of the "nonequilibrium" in the orthorhombic phase. A comparison of the calculated hyperfine magnetic fields (Table 4) with the

experimental values (12.7 and 12.3 T) (Table 3) demonstrates that the best agreement with the experimental data is observed when the iron atoms are located in the manganese sublattice of the orthorhombic ferromagnetic phase. In this case, we have $H_{\mathrm{hf},2a}^{\mathrm{VWN}} = 13.5$ T and $H_{\mathrm{hf},2c}^{\mathrm{VWN}} = 20.5$ T.

4. CONCLUSIONS

All the studied alloys $MnNi_{1-x}Fe_xGe$ ($0.10 \leqslant x \leqslant 0.25$) at $T = 290$ K are single-phase solid solutions with a hexagonal structure of the Ni2In type. In the temperature range from 70 K to the magnetic phase transition temperature T_C (slightly below room temperature), the solid solutions studied in this work are ferromagnets. The magnetic properties of the quenched and annealed samples of the $MnNi_{1-x}Fe_xGe$ alloys with iron concentrations in the range $0.10 \leqslant x \leqslant 0.25$ are almost independent of the type of heat treatment.

In the $MnNi_{1-x}Fe_xGe$ solid solutions with iron concentrations $x \sim 0.10$–0.15, the iron atoms are statistically distributed over structurally nonequivalent positions of two types, namely, MeI and MeII. At iron concentrations $x > 0.15$, the iron atoms replace the manganese atoms in the MeI positions. The nickel atoms in the MeII positions are not replaced by the iron atoms.

REFERENCES

1. E. H. Brück, O. Tegusi, and F. R. De Boer, US Patent 7069729 B2 (2004).
2. E. Liu, W. Wang, L. Feng, W. Zhu, G. Li, J. Chen, H. Zhang, G. Wu, C. Jiang, H. Xu, F. de Boer, Nat. Commun. **3**, 873 (2012).
3. L. Chen, F. X. Hu, J. Wang, L. F. Bao, J. R. Sun, B. G. Shen, J. H. Yin, and L. Q. Pan, Appl. Phys. Lett. **101**, 012401 (2012).
4. S. C. Ma, H. C. Xuan, C. L. Zhang, L. Y. Wang, Q. Q. Cao, D. H. Wang, and Y. W. Du, Appl. Phys. Lett. **97**, 052506 (2010).
5. V. I. Mitsiuk, T. M. Tkachenka, M. Budzy'nski, Z. Surowiec, and V. I. Valkov, Nukleonika **58**, 169701 (2013).
6. A. Szytula, A.T. Pędziwiatr, Z. Tomkowicz, and W. Bazela, J. Magn. Magn. Mater. **25**, 176 (1981).
7. M. R. L. N. Murthy, M. G. Natera, R. J. Begum, and N. S. Satya Murthy, in Proceedings of the Nuclear Physics and Solid State Physics Symposium, Bombay, February 1–4, 1972, p. 513.
8. C. L. Zhang, D. H. Wang, J. Chen, T. Z. Wang, G. X. Xie, and C. Zhu, Chin. Phys. B **20**, 097501 (2011).
9. C. L. Zhang, D. H. Wang, Q. Q. Cao, S. Ma, H. Xuan, and Y. Du, J. Phys. D: Appl. Phys. **43**, 205003 (2010).
10. A. D. Bruce and R. A. Cowley, Structural Phase Transitions (Taylor and Francis, London, 1981). 326 p.
11. J. Łażewski, P. Piekarz, and K. Parlinski, Phys. Rev. B: Condens. Matter **83**, 054108 (2011).
12. G. K. Wertheim, V. Jaccarino, and J. H. Wernick, Phys. Rev. [Sect.] A 135, A151 (1964).
13. H. Ebert, Munich SPRKKR package v.6.3. http://olymp.cup.uni-muenchen.de/.
14. S. H. Vosko, L. Wilk, and M. Nusair, Can. J. Phys. **58**, 1200 (1980).
15. J. P. Perdew, K. Burke, and M. Ernzerhof, Phys. Rev. Lett. **77**, 3865 (1996).

Translated by O. Borovik-Romanova

SPELL: OK